

Dynamics and Variance Control of Hot Mill Loopers

Sansal K. Yildiz, Biao Huang ^{*}, J. Fraser Forbes

*Department of Chemical and Materials Engineering, University of Alberta,
Edmonton, Alberta, Canada T6G 2G6*

Abstract

Poor control of hot strip mill loopers degrades strip width and gauge, and may even lead to mill breakdowns due to instability. In this study, dynamics of the looper-strip system and the control challenges it poses are discussed, and covariance control theory is applied to variance control design for loopers. Since looper disturbances have a deterministic nature, and their accurate modelling is a challenge that is not easily addressed, the problem represents a case in which a variance controller has to be designed without an explicit disturbance model. Control performance is assessed on a full-stand, nonlinear high fidelity finishing mill simulator, and comparisons to a conventional control system are provided.

Key words: Loopers, Covariance control, Variance control, Hot strip mill, Hot rolling

1 Introduction

A finishing mill produces thin sheet from hot steel bars by successively reducing the gauge using 5 to 7 sets of rolls, each called a mill stand. The finishing mill is part of a hot strip mill, of which a typical layout is given in Figure 1. Those units of the hot mill located before the finishing mill are responsible for reheating the cast slab, effecting the major gauge reduction (roughing), and finally transferring the workpiece (now called a transfer bar) to the finishing mill. After the finishing, the strip is cooled and coiled.

It is the finishing mill where a smaller but more precise gauge reduction is carried out. The strip emerging from a finishing mill can be as thin as 1.5

^{*} Corresponding author.

Email address: biao.huang@ualberta.ca (Biao Huang).

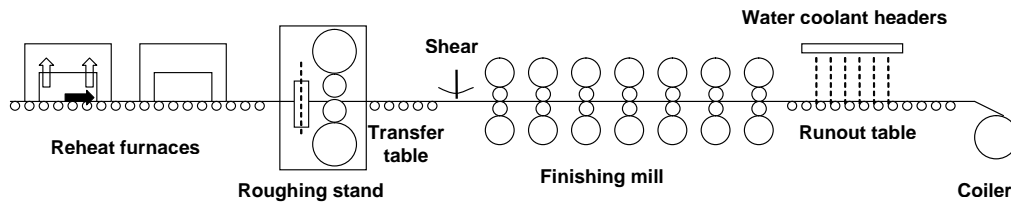


Fig. 1. Layout of a semi-continuous hot strip mill with 1 reversing rougher mm or even less, and its length may well exceed a kilometer. While the strip properties such as centerline gauge, width, profile and temperature must be precisely controlled to meet product requirements, these properties are only measured either at the entry or exit of the finishing mill in many plants, mainly because of the maintenance problems caused by the extreme environment of the finishing mill.

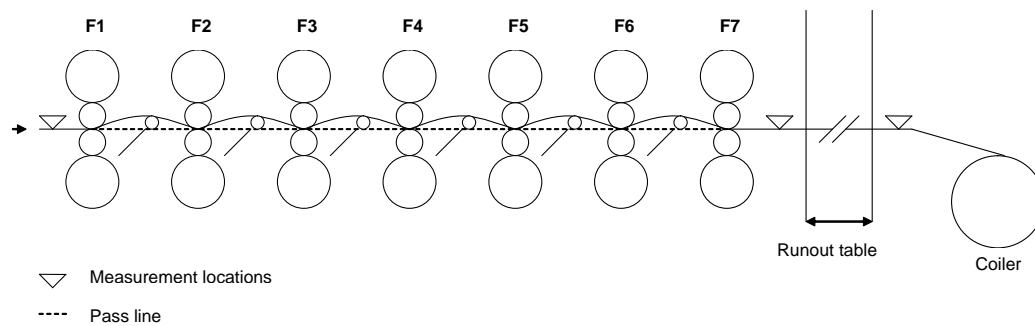


Fig. 2. Layout of a 7-stand finishing mill

Dimensions of hot and thin strip, especially the width, are sensitive to tension variations. The tension variations are inevitable in tandem mills, because the roll rotation speeds cannot be regulated with sufficient precision. In order to add a degree of freedom that prevents abrupt tension changes, and to serve as a sensitive indicator of tension variations, loopers are used. These are depicted

in Figure 2 in their installed positions. The looper is a roll on a pivot arm which lifts the strip, and is generally driven by an electric motor, although hydraulic or pneumatic drives also exist (Clark et al., 1997). Tension variations cause the looper to deviate from the nominal operating angle, from which the direction and magnitude of the variation can be inferred. In order to maintain a stable operation, looper controllers should be designed so that the loopers remain within a certain range around their operating point.

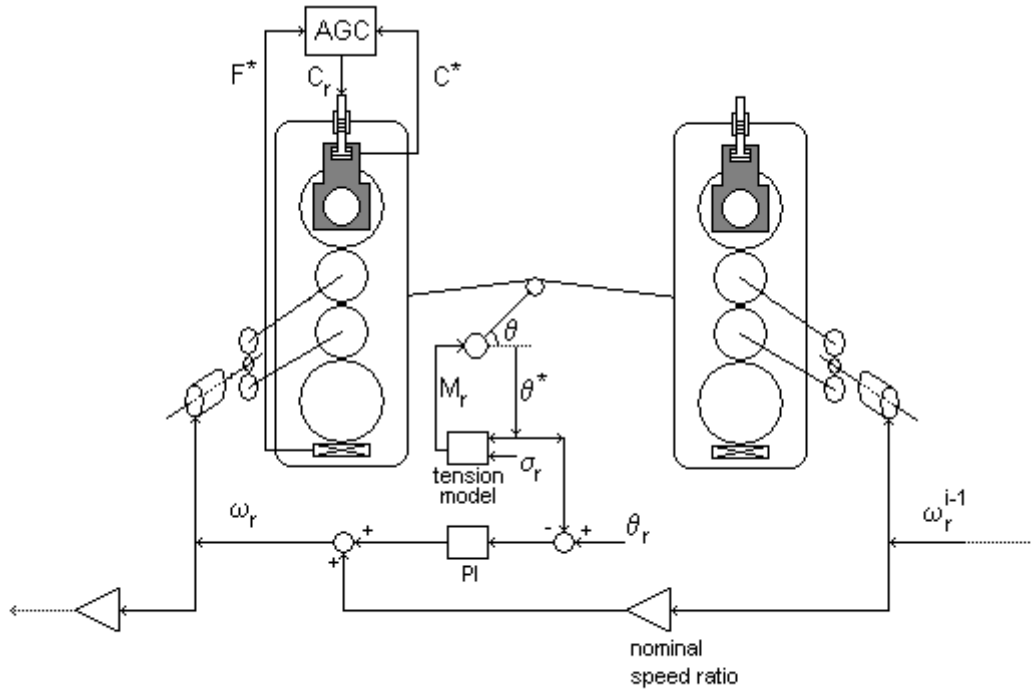
An earlier treatise of the loopers, the related hot mill equipment, and conventional looper control was given by Price (Price, 1973). Due to an increasing demand in tighter strip dimensional tolerances, the last two decades have witnessed many modern control designs, both commissioned and uncommissioned, in the area of looper control. Examples are Imanari et al.'s H-infinity (Imanari et al., 1997) and ILQ (inverse linear quadratic) (Imanari et al., 1998) controllers, Seki et al.'s optimal controller (Seki et al., 1991), Okada et al.'s optimal controller (Okada et al., 1998), and Hearns and Grimble's robust controllers (Hearns and Grimble, 2000), the latter two designs combining looper control and gauge control. A critical and more complete account of the recent developments in looper control can be found in Choi et al.'s survey paper (Choi et al., 2007). An excellent review on modern hot rolling process control in general has been written by Takahashi (Takahashi, 2001). Some most recent work can be found in (Furlan et al., 2007) and (Marcu et al., 2007).

In this paper, application of covariance control theory to the looper variance control problem is studied. Covariance control is an optimal control method that aims to keep the covariances of the output variables within specified design constraints while minimizing certain objective functions such as the input energy. An algebraic approach to control design and a comparison of covariance control to other control methods can be found in (Grigoriadis, 1998). Once the design requirements for output covariances are specified, a covariance controller can be easily designed for regulation problems provided that an accurate disturbance model is available; however, it is difficult to obtain an accurate disturbance model for the looper control problem due to a lack of measurements. This paper presents a case in which the covariance control theory is applied to a regulation problem with inadequate knowledge of the disturbance.

2 The control problem

Schematic descriptions of the conventional regulator structure and the stand-looper system can be found in Figures 3 and 4, respectively.

The looper control task can be summarized as minimizing the fluctuations



(*) indicates a measurement

Fig. 3. The conventional regulator structure

in looper angle (θ) and strip tension (σ) through manipulation of roll speed reference (ω_r) and looper motor torque reference (M_r). To achieve this task, the conventional control system outlined in Figure 3 employs two loops: the PI-based angle control loop, which manipulates the roll speed based on angle feedback; and the tension control loop, which sets the looper torque required to produce the reference tension. The tension controller is essentially a nonlinear, static model that calculates the required amount of torque at any given looper angle. In some installations, loop length is the controlled variable instead of the looper angle, and it is inferred from looper angle via a nonlinear model. Note the speed feedforward loop that adds the scaled downstream speed correction to that of upstream in order to decouple the looper from the downstream looper's controller.

2.1 Plant model

A linear dynamic model for the plant with actuators can be obtained by simplifying and linearizing the related equations of the detailed finishing mill model given in (Yildiz, 2005) or directly from the literature (Hearn and Grumble, 2000). An outline of the model in (Yildiz, 2005) is as follows. When applied to the looper-strip system, Newton's law of motion yields:

$$J\ddot{\theta} = M - M_L - c_v\dot{\theta} \quad (1)$$

where J is the total inertia of the looper and strip, M the motor torque on the looper, M_L the load on the looper, and c_v a viscous friction coefficient. The inertia (J) changes slightly with the looper angle. The load (M_L) is a combination of the loads caused by strip tension, strip weight, the looper's own weight and the force required to bend the strip. The major contribution is most often due to strip tension load, which can be expressed as:

$$M_\sigma = \sigma w \bar{h} [(-\cos \alpha_L + \cos \alpha_R)(l \sin \theta + r_l) + (\sin \alpha_L + \sin \alpha_R)(l \cos \theta)] \quad (2)$$

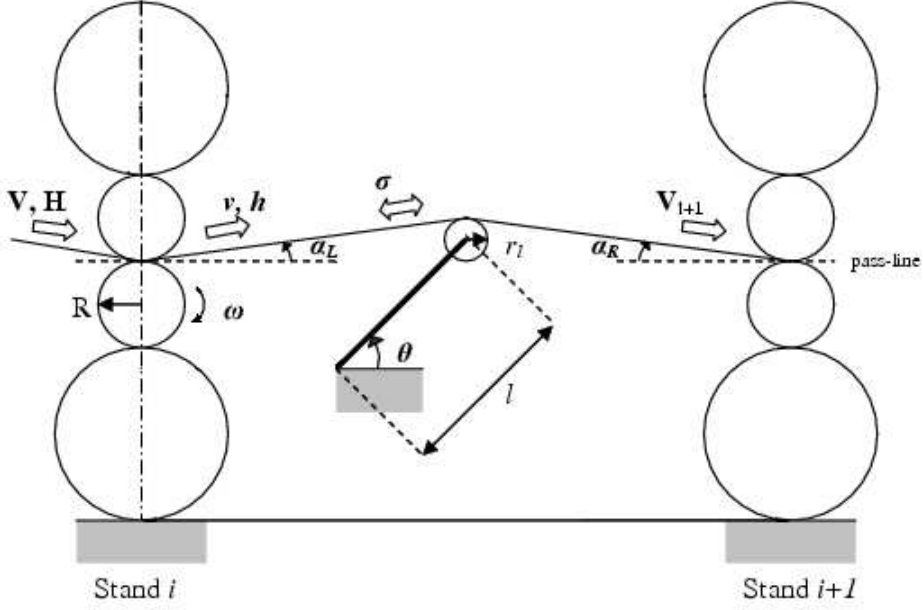


Fig. 4. A schematic drawing of the stand-looper system

In Equation (2), w is the strip width, \bar{h} is the nominal strip gauge, and the rest are as shown in Figure 4. Note that the right and left strip angles (α_R, α_L) depend on the looper angle only. The rate of tension change can be derived from Hooke's law and a consideration of the rate of inter-stand strip consumption:

$$\dot{\sigma} = \frac{E}{L} \left(\frac{dL}{d\theta} \dot{\theta} - v + V_{i+1} \right) \quad (3)$$

where E is the strip modulus of elasticity; L is the strip length; v is the de-threading speed of Stand i ; and V_{i+1} is the threading speed of Stand $i + 1$.

The strip speed imbalance term in Equation (3) can be expanded as:

$$V_{i+1} - v = w - \Delta\omega R(1 + \bar{f}) - \bar{\omega} R \frac{\partial f}{\partial \sigma} \Delta\sigma \quad (4)$$

while the threading speed has the relation:

$$V_{i+1} = \frac{v_{i+1}h_{i+1}}{H_{i+1}} = \omega_{i+1}R_{i+1}(1 + f_{i+1})\frac{h_{i+1}}{H_{i+1}} \quad (7)$$

The slip factor (f) in Equations (6) and (7) accounts for the speed difference between the roll surface and the strip. As this slip is mainly a function of entry and exit gauges (H, h), it can be concluded from Equations (6) and (7) that gauge variations are a major cause of the speed imbalance. The reasons for the gauge variation, therefore, become of interest.

In a finishing mill, the gauge fluctuation is primarily because of non-uniform transfer bar temperature, which affects the steel hardness. Non-uniform transfer bar gauge also has an affect, mostly at the earlier stands. Temperature and gauge variations are usually of periodic nature and occur at low frequencies. Spectral analysis of a typical entry temperature profile is provided in Figure 5 as an example. Misaligned or imperfectly round mill rolls also cause periodic gauge variations, smaller in size but at much higher frequencies (0.5 Hz - 5 Hz and harmonics). Another low-frequency disturbance on the looper-strip system is introduced by flatness defects such as edge waves or centre buckles, but such effects cannot be properly described using one-dimensional control models such as the one in Equation (5).

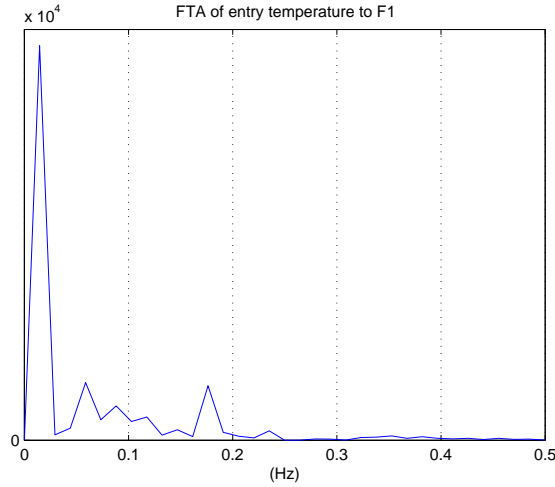


Fig. 5. Fourier transform analysis of entry temperature to Stand 1

Finishing mills are equipped with an automatic gauge control (AGC) system on each stand, of which a grossly-simplified scheme is provided in Figure 3. Although usually quite complex, AGCs in essence use the roll force F^* and roll position C^* measurements to create a roll position change signal C_r that compensates for the aforementioned disturbances and regulates the exit gauge. While they have a regulatory effect on the de-threading speed, AGCs often upset the threading speed, thus producing an unfavourable overall impact on the

loopers. Especially the hydraulic AGCs, which have replaced the slow-response electromechanical screws in many mills, run a serious risk of destabilizing the loopers.

2.3 Looper-Strip frequency response

An inspection of the looper-strip system's disturbance sensitivity gives important hints as to the achievable control performance. Sensitivities of both looper angle and strip tension to speed disturbance are shown in Figure 6 for strip dimensions that are typical for Loopers 1 and 6 of a finishing mill.

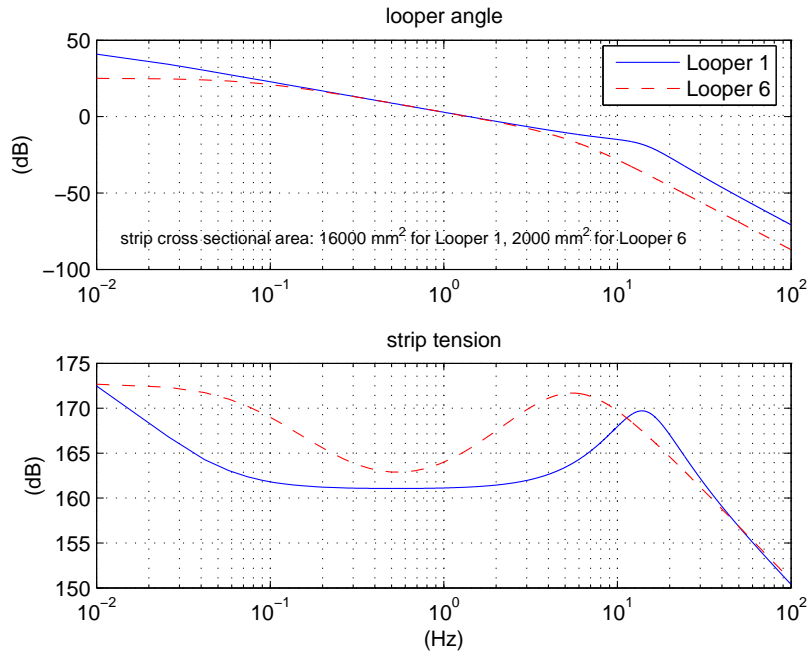


Fig. 6. Sensitivities of Loopers 1 and 6 to speed disturbance

Figure 6 reveals that the looper-strip system has a resonance point in the high frequency region around which strip tension becomes very sensitive to the disturbance. The resonance frequency mainly depends on strip cross sectional area, which can be shown via the approximate equation (Yildiz, 2005):

$$\omega_n = \sqrt{\frac{whE}{J}}\varphi_0 \quad (8)$$

where φ_0 is only a function of stand-looper structure. Thus, due to the continual gauge reduction, the highly sensitive region must shift to lower frequency ranges as the looper number increases, as illustrated in Figure 6, while the roll speed ranges must move to higher frequencies. The two ranges often overlap

in the case of later loopers, leading to substantial tension variations due to roll eccentricity.

Responses of the main drives are typically not quick enough to exercise effective control around and above the resonance frequencies, where the closed-loop sensitivity is often identical to the open-loop, or could even be higher if the looper controller is not properly tuned.

2.4 Conventional looper control design

As noted in Section 2, the conventional system uses two independent loops to control the angle and the tension. The tension controller can be easily constructed from a static tension model of the form in Equation (2). Thus, at any given looper angle and tension reference, the torque reference signal will be calculated using the nonlinear model: $M_r = M(\theta, \sigma_r)$. In practice, a low-pass filter is also included in the loop to prevent the noise in the angle measurement from directly going into the torque reference.

For the PI-based angle controller design it should be sufficient to consider the main drive dynamics only, since the looper dynamics are faster and would be outside the effective band of the PI controller. Hence, instead of Equation (5), a simpler equation neglecting the looper dynamics can be used for the design work:

$$\frac{\Delta\theta(s)}{\Delta\omega_r(s)} = \frac{k}{s(T_{md}s + 1)} \quad (9)$$

where the constant k is equal to $d\theta/dL R_0(1 + \bar{f})$; the lag represents the main drive dynamics, and the integrator converts speed into length.

Wang and Cluett's PID design procedure for integrating systems (Wang and Cluett, 1997) is a suitable method for the system in Equation (9). This tuning method is based on selection of the parameters β and ζ for shaping the desired controller response, which is expressed as:

$$G_{ru}(s) = \frac{s(2\zeta\tau + \gamma_1)s + 1}{K\tau^2s^2 + 2\zeta\tau s + 1} \quad (10)$$

The natural period τ of the desired controller signal is selected as $\tau = \beta\gamma_1$ where γ_1 is the second coefficient of the Taylor series expansion of the integrating process G_I around $s = 0$:

$$G_I(s) = \frac{K}{s}(1 + \gamma_1s + \dots) \quad (11)$$

Thus, β can be used to adjust the speed of the control signal. For lag dominant processes, which are defined by $\gamma_1 < 0$, it is recommended the damping factor ζ be selected as either $1/\sqrt{2}$ or 1. Then, the PID controller is found by dividing the desired open-loop transfer function $G_{ol}(s)$ by process transfer function $G_I(s)$ and fitting the result to a PID controller form in the frequency domain. This procedure can be summarized as follows:

$$G_{ol}(s) = \frac{G_{ru}(s)G_I(s)}{1 - G_{ru}(s)G_I(s)} \quad (12)$$

$$c_2(j\omega)^2 + c_1(j\omega) + c_0 \approx \frac{G_{ol}(j\omega) \times j\omega}{G_I(j\omega)} \quad (13)$$

The two frequencies ω_1 and ω_2 necessary to calculate the constants c_0, c_1, c_2 in Equation (13) are selected as $2\pi/T_s$ and $4\pi/T_s$, T_s being the desired closed-loop process output settling time. The controller gain and the integral time constants are then simply $K_c = c_1$ and $\tau_I = c_1/c_0$.

In this particular design problem, values of the plant time constant and natural period of the controller are equal for $\beta = 1$. Since it is desirable for stability considerations that a PI controller should have a slower response than the actuator, $\beta = 1$ and higher values are ideal starting points for the designer. Experience has shown that theoretically stable controllers can be designed with β values as low as 0.8; however, performance tests on the full-stand, non-linear finishing mill simulator indicate that such controllers are too aggressive for stable operation. $\beta = 2$ or $\beta = 3$ are required in many cases to maintain a smooth operation. Simulated performances of conventional control systems tuned as described above can be found in Section 4.

3 Covariance control

The covariance control design task may be described as designing a dynamic output feedback controller:

$$\dot{x}_c = A_c x_c + B_c z \quad (14)$$

$$u = C_c x_c \quad (15)$$

for the plant:

$$\dot{x} = Ax + B_u u + B_w w \quad (16)$$

$$y = C_y x \quad (17)$$

$$z = C_z x + v \quad (18)$$

so that the covariance/variance constraints:

$$\lim_{t \rightarrow \infty} E(\mathbf{y}\mathbf{y}^T) \leq Y \quad (19)$$

$$\lim_{t \rightarrow \infty} E(\mathbf{u}^T \mathbf{R} \mathbf{u}) \leq \min \gamma \quad (20)$$

are satisfied. In the equations above, \mathbf{y} is the vector of controlled outputs; \mathbf{z} is the vector of measurements; \mathbf{w} and \mathbf{v} are white noise vectors with intensity matrices W and V , representing the disturbance and measurement noise, respectively. Note that matrix Y in Equation (19) is simply an output covariance constraint and the scalar bound γ is the minimal control energy satisfying the output covariance constraint. The controlled variables must of course either be measured or observable for the covariance controller to be feasible.

It is possible to solve the covariance control problem using linear matrix inequalities (LMIs). Feasibility of the controller in Equations (14) and (15) that stabilizes the plant and satisfies all design requirements is equivalent to the existence of some matrices satisfying a set of LMIs (Huang et al., 2004). This design method proposed by (Huang et al., 2004) ensures the global optimality of the controller.

3.1 *Looper variance control*

The looper variance control problem can easily be cast into the frame of the covariance control problem explained in Section 3. The first step is to augment the plant in Equation (5) with two integrating states so that:

$$\dot{\mathbf{x}} = \begin{bmatrix} A & 0 \\ I & 0 \end{bmatrix} \mathbf{x} + \begin{bmatrix} B_u \\ 0 \end{bmatrix} \mathbf{u} + \begin{bmatrix} B_w \\ 0 \end{bmatrix} \mathbf{w} \quad (21)$$

where $\mathbf{x} = [x \ x_6 \ x_7]^T$, $\mathbf{u} = u$ and $\mathbf{w} = w$. This augmentation is necessary to be able to ensure high control gains in the low frequency region where the majority of the disturbance lies. The same effect could be obtained through proper modelling of the disturbance, which could in fact give a better disturbance rejection performance; however, in this particular case knowledge of the disturbance is inadequate. Furthermore, the disturbance characteristics change with the bar to be rolled, the rolling speed, and other mill conditions; so, many of the additional benefits that could be expected from careful modelling of a particular disturbance will not be realized when the disturbance changes.

The second step is to expand the output vector to include the integrated states, which then becomes:

$$y = C_y x = [\theta \ \sigma \ \int \theta dt \ \int \sigma dt]^T \quad (22)$$

Unlike the other states, x_6 and x_7 are not observable from the looper angle measurement because they have no influence on the looper angle. This requires the tension to be measured, in which case the measurement vector may include all the controlled variables. After the steps described above, a variance controller can be designed by specifying the diagonal elements of Y , W and V , and the control weight R .

Tension is not measured in many hot mills. In such cases it may be inferred from looper angle and looper torque measurements so that the variance controller can be implemented; however, with an inferential measurement, the output variance bounds cannot be guaranteed. Further, an inferential sensor will increase the complexity of the design. A simple alternative is to modify the augmented plant in Equation (21) so that the torque reference (M_r) is integrated instead of tension, i.e., $\dot{x}_7 = M_r$, and the control vector becomes:

$$y = [\theta \ \sigma \ \int \theta dt \ \int M_r dt]^T \quad (23)$$

The new augmented system is observable using looper angle and torque reference only. Note that the former is an available measurement and the latter is a controller output, and a tension measurement is no longer necessary. Indirect prevention of tension offset as explained above is justified by the fact that, when the dynamic effects are omitted, tension is only a function of looper angle and torque, i.e., $\sigma = f(\theta, M)$. Therefore, prevention of angle and torque offsets should prevent a tension offset.

3.2 Control design

The control design procedure involves specification of the parameters W , Y , V and R , calculation of the optimal controller by solving the appropriate LMIs, and finally refinement of the parameters to provide the desired closed-loop performance. A MATLAB code of (Zhang and Huang, 2003; Huang et al., 2004) was used for calculation of the controllers.

The main difficulty associated with not using a disturbance model appears when specification of W is attempted. In this particular problem there is only one disturbance input, and hence, W becomes a scalar indicating the variance of the white noise disturbance; however, it cannot be directly equated

to the variance of the speed disturbance because, as discussed before, the disturbance does not exhibit white noise characteristics and a disturbance model is not included in the plant model. Moreover, in this particular case, the variance of the speed disturbance is not accurately known. Consequently, the disturbance variance has to be treated as a tuning parameter, rather than the actual variance. Since there is a direct relationship between the disturbance and output variances, this means that it is no longer possible to directly use the design specifications for the allowable output variances as the variance constraint (Y). Some tuning will be necessary and it is important during the tuning to check step and frequency responses of the controller in order to establish a better connection to the actual performance. The advantage of control tuning based on covariance control theory is its ability to adjust performance of each output directly by tuning the variance upper bound on the corresponding output.

The broadband measurement noise intensity (V) can still be used to ensure high frequency roll-off of the controller response, even if the real measurement noise magnitude is unknown. As long as it is below a critical point, which can be iteratively determined, it effectively curtails high frequency control gains, while leaving the low frequency response essentially untouched. In this particular problem, R has little effect on controller outputs, due to reasons that will be discussed later.

Table 1

Variance control design parameters for Loopers 3 and 5

For Looper No	Design Parameters					
	W (m^2s^{-2})	$\text{var}(\theta)$ (rad^2)	$\text{var}(\sigma)$ (Pa^2)	$\text{var}(\int \theta dt)$ (rad^2s^2)	$\text{var}(\int \sigma dt)$ (Pa^2s^2)	$\text{var}(\int M_r dt)$ ($\text{N}^2\text{m}^2\text{s}^2$)
3	1×10^{-9}	1×10^{-8}	4×10^9	3.3×10^{-10}	N/A	4×10^{-6}
3*	1×10^{-9}	1×10^{-8}	4×10^9	3.3×10^{-10}	4×10^6	N/A
5	1×10^{-9}	9×10^{-9}	3×10^9	5×10^{-10}	N/A	4×10^{-6}
5*	1×10^{-9}	6×10^{-9}	1×10^9	3.3×10^{-10}	5×10^5	N/A

The design exercise has shown that, as expected, decreasing the output and integrated output variance bounds is equivalent to decreasing the high and low frequency closed-loop sensitivities, respectively. The parameters that were used for different designs are provided in Table 1, where the controllers that use tension feedback are distinguished from those with torque feedback with an asterisk placed next to the looper number. The closed-loop responses of these designs are plotted in Figures 7 and 8 together with the responses of a conventionally controlled system. In these figures, step responses are plotted on the left and the closed-loop frequency responses on the right. The conventional system was tuned on the simulator to give the fastest possible response without

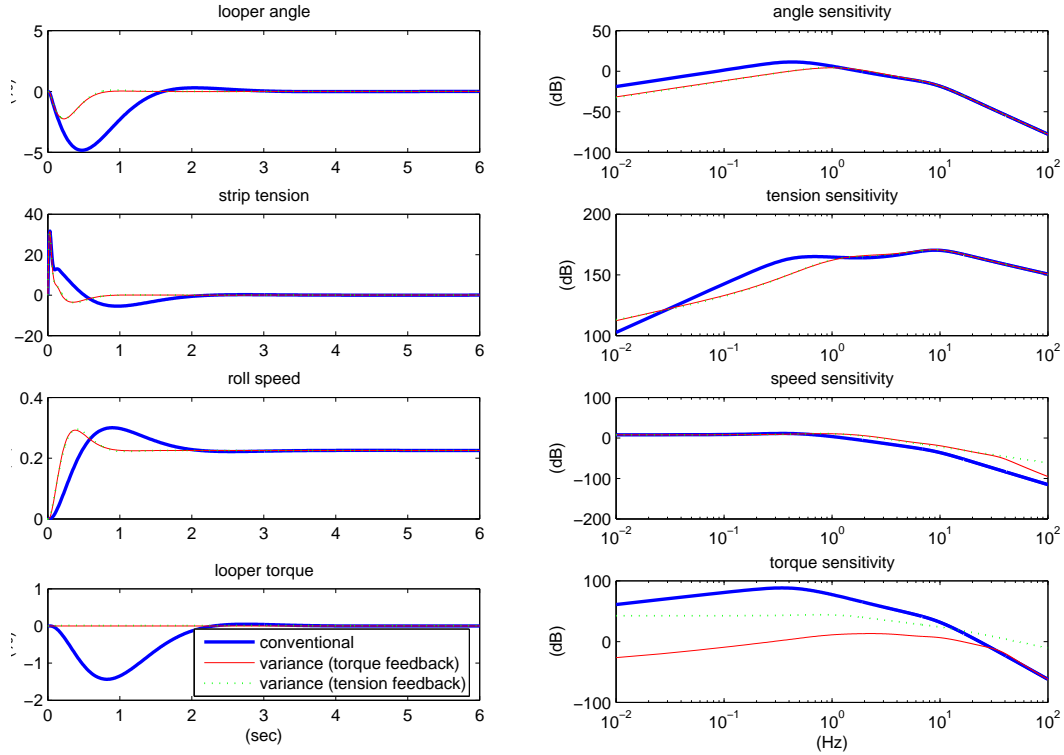


Fig. 7. Disturbance rejection performance for Looper 3

causing instability. Its response characteristics are of interest as they constitute a basis for performance comparison as well as a reference point for tuning of the variance controller.

The torque and tension feedback controllers of Looper 3 were designed using the identical design parameters in order to demonstrate the equivalence of the two design approaches. It can be verified from Figure 7 that the resulting performances are almost identical. The controllers were tuned such that the closed-loop sensitivities in the low-frequency region were substantially lower than that of the conventional controller. Remarkably, the sensitivities around and beyond the resonance point are very much the same for both variance and conventional control. This is in accordance with the previous observation that due to the looper-strip resonance and the slow response of the main drives, high frequency tension control through the loopers may not be feasible.

Although the resulting controller may not be practically useful due to its extreme control energy use, designing variance controllers with much lower high-frequency sensitivities is possible. This idea will be demonstrated for Looper 5. In Table 1 it can be observed that the tension-feedback controller of Looper 5 was designed for lower output variance constraints. The remarkable difference that resulted between the closed-loop sensitivities and control energy

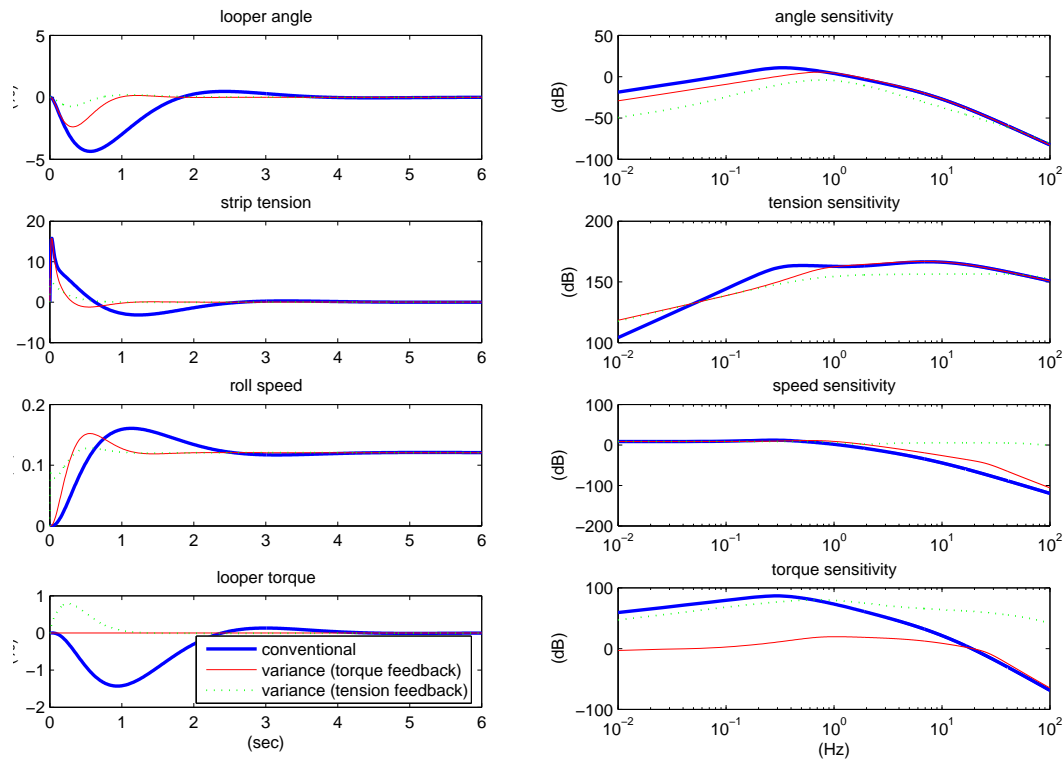


Fig. 8. Disturbance rejection performance for Looper 5

use can be seen in Figure 8. It is noteworthy that this sensitivity decrease could only be achieved with the tension feedback controller. The torque-feedback controller cannot satisfy the reduced bounds.

It has also been found during these tuning exercises that if the tuning is not properly carried out, the closed-loop tension sensitivity under a variance controller may be substantially higher around the resonance frequency than that of a conventional controller.

4 Simulation results

The controllers thus designed were tested on a nonlinear, high-fidelity finishing mill simulator which includes 7 mill stands and a coiler. The underlying nonlinear model and validation performance of this simulator were discussed in our previous work (Yildiz, 2005). The simulation accounts for the variable inter-stand transport delays, and incorporates detailed models of the AGC system and the main drives. A transfer bar temperature profile taken from real plant operation was used for the simulations as well as realistic amounts of roll eccentricity.

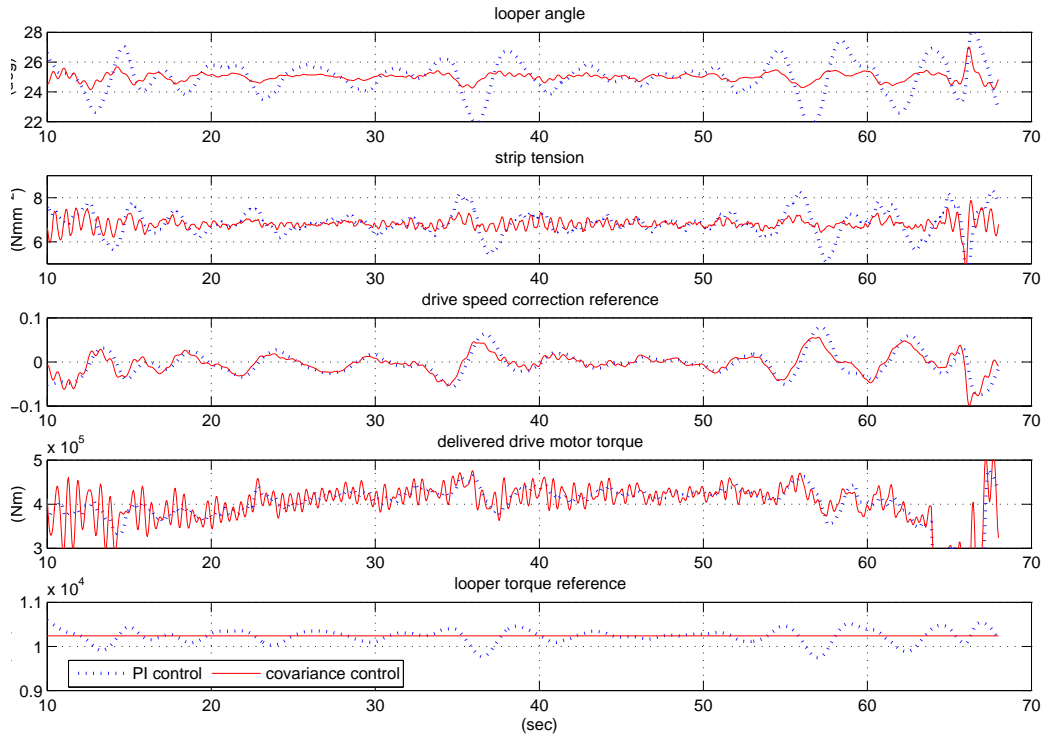


Fig. 9. Simulated conventional and variance control performance for Looper 3

Simulated performances of the conventional controller and the variance controller without tension feedback on Looper 3 are shown in Figure 9. Plots of the manipulated and controlled variables are provided as well as the main drive motor torque, since the motor torque is a more direct indicator of the control energy. The results provided in Figure 9 show a substantially better performance in the case of variance control: the angle variations are much smaller, reducing the risk of instability to a great extent, and the tension ranges within a narrower bound. The high frequency variations are due to roll eccentricity and are not as noticeable in the case of conventional control since it has a slightly lower closed-loop sensitivity in the high frequency region, as can be seen in Figure 7.

Similar comments can be made for a comparison of the variance and conventional control performances on Looper 5. In Figure 10, operation once again promises better stability, and the tension varies within a narrower band, while the variation due to eccentricity is slightly larger than that of the conventional control. Also note that the eccentricity effects are much more pronounced in general compared to the case of Looper 3, due to the smaller resonance frequency of Looper 5. Thus, the case poses a good opportunity to test the tension feedback controller that was designed in Section 3.2 for better high-frequency control. The results are provided in Figure 11 and indicate that the

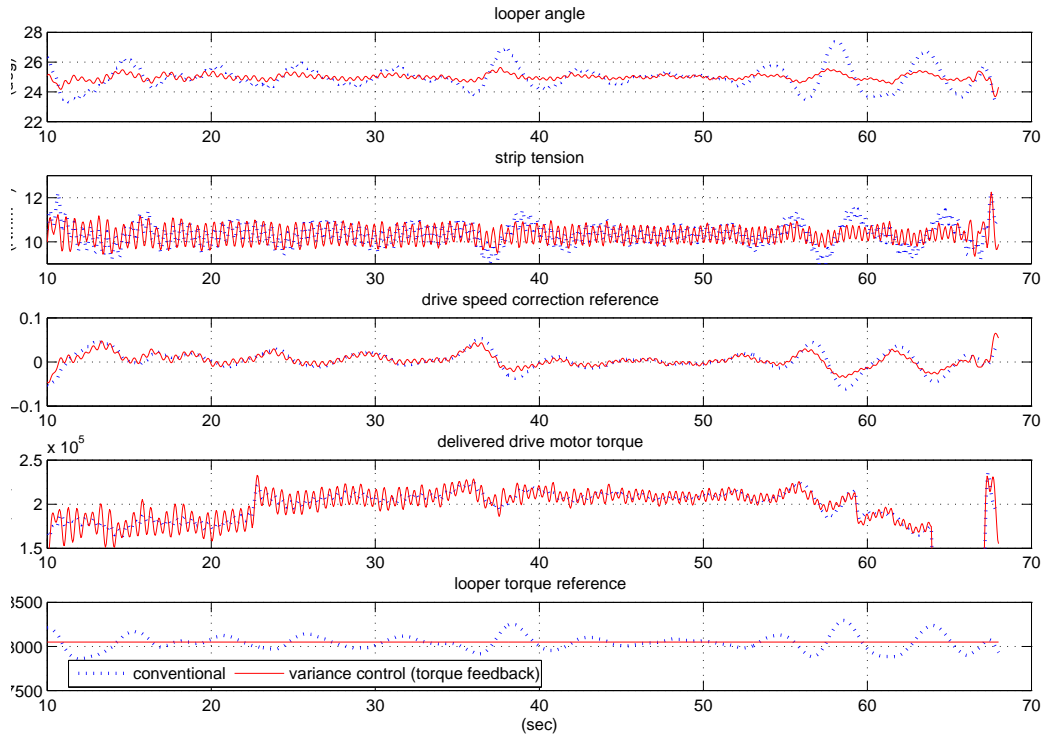


Fig. 10. Simulated conventional and variance control performance for Looper 5
eccentricity-induced tension variations can be suppressed to a level below that
of the conventional at the expense of greater drive torque use.

A final point is the variance controller’s virtually negligible use of the looper torque input. The fact that this behaviour cannot be visibly altered by modifying the control weight R suggests that the two inputs are not interchangeable. Indeed it can be verified through a qualitative analysis of the looper-strip system that most often the roll speed can be manipulated in a direction that has a corrective effect on both angle and tension, while the looper torque change often causes one of the variables to further deviate. Also interesting in Figure 11 is that the variance controller applies the torque in the opposite direction in comparison to the conventional controller; hence, using it to regulate the angle rather than the tension.

5 Conclusion

It has been found that covariance control theory can be successfully applied to regulator design problems for which an adequate model of the disturbance is not available. Absence of a disturbance model has prevented direct use

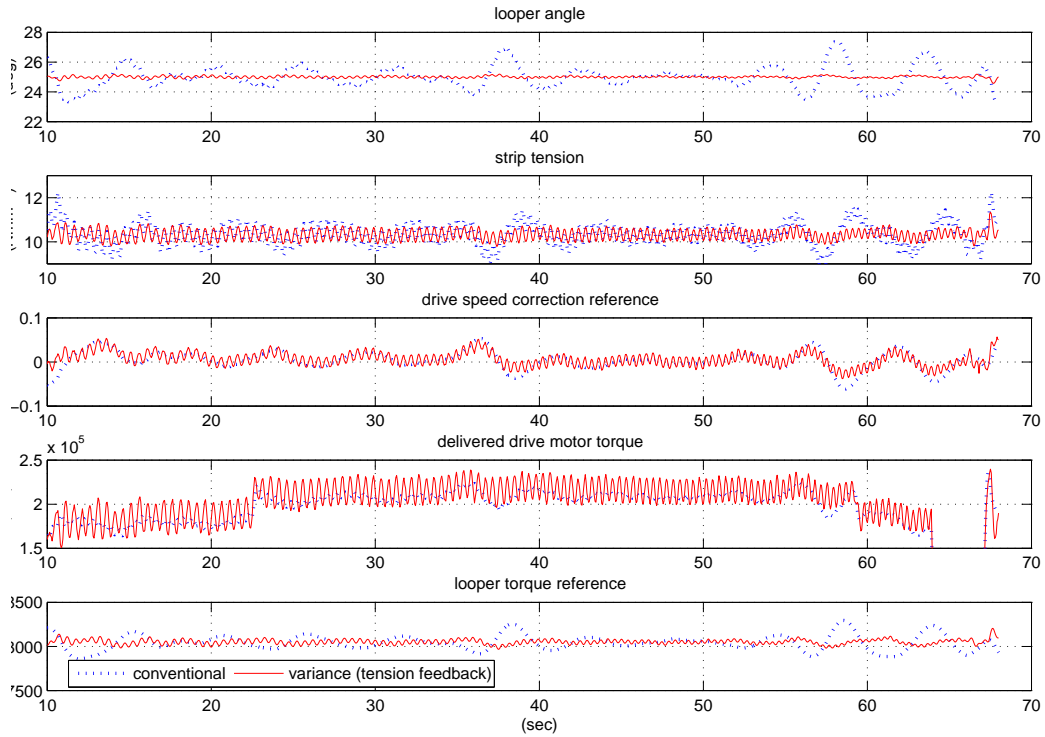


Fig. 11. Performance improvement for Looper 5 in case of narrower variance bounds and tension feedback

of the design specifications as the control design constraints, but through well-coordinated use of the error and integral error variance constraints and measurement noise levels, it has been possible to conveniently shape the closed-loop sensitivity and design high-performance looper control. The resulting controller is low-order, optimal in its control use, and integral in the sense that observer and feedback gains are synthesized in a single design.

A noteworthy observation is that when an integrating state for a variable needs to be added and controlled, a measurement of this variable must be available to overcome the observability problem. This stems from the fact that even if the variable itself is observable from a certain measurement, its integral will not be observable. This problem could be avoided in some cases by careful selection of the integrated variable to be controlled, as has been done for the looper control problem in this study.

The findings suggest that variance control can achieve substantially better performance compared to conventional control in terms of minimizing the output variations and, consequently, providing a more stable looper operation. Nevertheless, it should be tuned carefully to avoid large tension sensitivity around the resonance point, which will cause the roll eccentricity effects on

tension to be amplified, especially in case of later loopers.

The authors believe that the experience gained from this application is valuable in turning the covariance control theory into a powerful practical control design method.

Acknowledgments

The authors gratefully acknowledge the funding provided for this research by Dofasco Inc and the Natural Sciences and Engineering Research Council of Canada.

References

- Choi, I., Rossiter, A., Fleming, P., 2007. A survey of the looper-tension control technology in hot rolling mills. http://www.shef.ac.uk/content/1/c6/03/37/19/ifac_submit.pdf.
- Clark, M., Versteeg, H., Konijn, W., 1997. Development of new high performance loopers for hot strip mills. *IRON STEEL ENG* 74 (6), 64–70.
- Furlan, R., Cuzzola, A., Parisini, T., 2007. Friction compensation in the interstand looper of hot strip mills: A sliding-mode control approach. *CONTROL ENG PRACT*, doi:10.1016 In press.
- Grigoriadis, R. S. T. I., 1998. A unified algebraic approach to linear control design. Taylor & Francis.
- Hearn, G., Grimble, M., 2000. Robust multivariable control for hot strip mills. *ISIJ INT* 40 (10), 995–1002.
- Huang, X., Zhang, L., Huang, B., 2004. Stochastic lq control with generalized lq constraints. *DYN CONTIN DISCRET I*, 141–152.
- Imanari, H., Morimatsu, Y., Sekiguchi, K., Ezure, H., Matuoka, R., Tokuda, A., Otake, H., 1997. Looper H-infinity control for hot-strip mills. *IEEE T IND APPL* 33 (3), 790–796.
- Imanari, H., Seki, Y., Sekiguchi, K., Anbe, Y., 1998. Application of ILQ control theory to steel rolling process. Proceedings of the 7th International Conference on Steel Rolling, Chiba, Japan, *ISIJ*, 36–41.
- Isei, Y., Honda, T., Kimura, K., Yakita, Y., Buei, Y., 2004. Development of interstand velocimeter for hot strip finishing mill. *TETSU TO HAGANE* 90, 44–50.
- Marcu, T., Koppen-Seliger, B., Stucher, R., 2007. Design of fault detection for a hydraulic looper using dynamic neural networks. *CONTROL ENG PRACT*, doi:10.1016 In press.
- Okada, M., Murayama, K., Urano, A., Iwasaki, Y., Kawano, A., Shiomi, H.,

1998. Optimal control system for hot strip finishing mill. CONTROL ENG PRACT 6 (8), 1029–1034.
- Price, J., 1973. The hot strip mill looper system. IEEE T IND APPL 9 (5), 556–562.
- Seki, Y., Sekiguchi, K., Anbe, Y., Fukushima, K., Tsuji, Y., Ueno, S., 1991. Optimal multivariable looper control for hot strip finishing mill. IEEE T IND APPL 27 (1), 124–130.
- Takahashi, R., 2001. State of the art in hot rolling process control. CONTROL ENG PRACT 9 (9), 987–993.
- Wang, L., Cluett, W., 1997. Tuning PID controllers for integrating processes. IEE P-CONTR THEOR AP 144 (5), 385–392.
- Yildiz, S., 2005. Hot strip mill modeling and looper control. Master’s thesis, University of Alberta.
- Zhang, L., Huang, B., 2003. An LMI approach to sub-minimum energy control with output covariance constraints. Internal Report, University of Alberta.